Journal of Chromatography A 1711 (2023) 464463

Contents lists available at ScienceDirect

Journal of Chromatography A

journal homepage: www.elsevier.com/locate/chroma

Column-free optical deconvolution of intrinsic fluorescence for a monoclonal antibody and its product-related impurities

Deniz Uçan [a], John E. Hales [a], Samir Aoudjane [a], Nathan Todd [b], Paul A. Dalby [a,*]

[a] Department of Biochemical Engineering, Bernard Katz Building, University College London, Gower Street, London WC1E 6BT, UK
[b] Cytiva, 5 Harbourgate Business Park, Southampton Road, Portsmouth PO6 4BQ, UK

ARTICLE INFO

Keywords:
Analytical instrumentation
Process analytical technology
Antibody
Time-resolved intrinsic fluorescence
Biophysics

ABSTRACT

The quantification of monoclonal antibody (mAb) aggregates and fragments using high pressure liquid chromatography-size exclusion chromatography (HPLC-SEC) typically requires off-line measurements that are time-consuming and therefore not compatible with real-time monitoring. However, it has been crucial to manufacturing and process development, and remains the industrial standard in the assessment of product-related impurities. Here we demonstrate that our previously established intrinsic time-resolved fluorescence (TRF) approach can be used to quantify the bioprocess critical quality attribute (CQA) of antibody product purity at various stages of a typical downstream process, with the potential to be developed for in-line bioprocess monitoring. This was directly benchmarked against industry-standard HPLC-SEC. Strong linear correlations were observed between outputs from TRF spectroscopy and HPLC-SEC, for the monomer and aggregate-fragment content, with R^2 coefficients of 0.99 and 0.69, respectively. At total protein concentrations above 1.41 mg/mL, HPLC-SEC UV-Vis chromatograms displayed signs of detector saturation which reduced the accuracy of protein quantification, thus requiring additional sample dilution steps. By contrast, TRF spectroscopy increased in accuracy at these concentrations due to higher signal-to-noise ratios. Our approach opens the potential for reducing the time and labour required for validating aggregate content in mAb bioprocess stages from the several hours required for HPLC-SEC to a few minutes per sample.

1. Introduction

The number of monoclonal antibody (mAb) based therapeutics reaching late-stage development have more than doubled over the last decade [1] as they deliver high target specificity to cellular targets such as to tumour-specific antigens for a controlled immune response or to deliver cytotoxic payloads as antibody-drug conjugates [2].

During manufacturing of mAbs, undersired aggregates and fragments can form that are characterised by their particle size distribution, reversibility, solubility, and extent of denaturation. The potential immunogenicity of aggregate species renders them crucial for removal, and as such they form a key critical quality attribute (CQA) [3]. Various purification stages can expose the mAb to wide ranges of pH, protein concentrations, ionic strengths and surface interactions, that can lead to aggregation and fragmentation [4]. The low pH used for elution after Protein A capture and for viral inactivation are a particular point of risk for aggregation [5,6] and fragmentation due to peptide-bond hydrolysis, especially within the hinge-region [7,8]. The presence of proteases in the milieu of host-cell proteins (HCPs) can also digest accessible peptide bonds to yield Fab and Fab-Fc fragments [9,10]. Such fragments can compromise the overall pharmaceutical efficacy [11–13], immunogenicity and chemical stability of the formulated product [14].

Analysis and quantification of product-related impurities in industry is most commonly achieved using high performance liquid chromatography size exclusion chromatography (HPLC-SEC) [15]. Analytical HPLC-SEC is typically performed after Protein A chromatography to minimise fouling and interference from cell culture components and HCPs from earlier stages [16–18]. However, its analytical accuracy can still be impacted by non-specific binding of aggregates [15,19]. Additionally, SEC analysis may sometimes require a dilution step before sample injection to avoid detector and column saturation. This can often dissociate reversible aggregates, making the results less reliable. Furthermore, the dynamic range of molecular masses that can be adequately resolved is limited by column pore size, such that selecting a column and conditions for an acceptable separation of monomers and dimers, would lead to reduced estimations of larger aggregates [20].

* Corresponding author.
E-mail address: p.dalby@ucl.ac.uk (P.A. Dalby).

https://doi.org/10.1016/j.chroma.2023.464463
Received 24 July 2023; Received in revised form 12 October 2023; Accepted 17 October 2023
Available online 18 October 2023

Fig. 1. Flow diagram of the bioprocess stages for mAb manufacture. Eluates were from Protein A capture chromatography, viral inactivation, cation exchange, anion exchange and ultrafiltration.

Table 1
Summary of the decay parameters extracted from the FPLC SEC-TRF DC plots for the main species in each sample for each bioprocess stage that was analysed.

Test regimen	Bioprocess stage	Species class	Decay parameters		
			β	τ_1 [ns]	τ_2 [ns]
Original sensitivity, *high* concentration (4.70 mg/mL > total protein concentration > 1.41 mg/mL) Low laser pulse power: 40μJ	Protein A, Viral inactivation	Monomer	0.384	1.35	4.97
		Aggregate/ fragment	0.281	0.952	5.20
	S HyperCel	Monomer	0.343	1.35	5.43
		Aggregate/ fragment	0.340	1.04	5.27
	Mustang Q	Monomer	0.329	1.32	5.37
		Aggregate/ fragment	0.317	0.905	4.63
	Ultrafiltration	Monomer	0.251	0.923	4.82
		Aggregate/ fragment	0.220	0.750	3.62
Original sensitivity, *low* concentration (1.10 mg/mL > total protein > 0.31 mg/mL) Low laser pulse power: 40 μJ	Ultrafiltration	Monomer	0.251	0.923	4.82
		Aggregate/ fragment	0.260	0.647	5.02
Sensitivity-improved (2.82 mg/mL > total protein > 0.28 mg/mL) High laser pulse power: 50 μJ	Mustang Q	Monomer	0.251	0.923	4.82
		Aggregate/ fragment	0.260	0.647	5.02

In-line spectroscopies that are capable of quantifying CQAs in real time, have the potential to enable a process analytical technology (PAT) framework, in which real-time analysis informs process control and the release of product with acceptable CQAs. Current bioprocess monitoring often relies on offline analytical chromatography such as SEC, and so methods that eliminate this chromatographic step could provide faster analyses of target and contaminant protein concentrations. Spectroscopic data for PAT is inherently multivariate, and so mathematical tools can enable a higher selectivity for CQA evaluation [21,22]. Earlier studies into the in-line analysis of protein species have used UV absorption spectra together with Partial Least Squares Regression (PLS) models to predict co-eluting protein quantities [23–25]. When combined with principal component analysis (PCA), direct comparisons of spectral similarity between proteins have been mapped to form an identification tool [26].

Intrinsic fluorescence intensity measurements has previously been used for protein detection in acrylamide gel and capillary electrophoresis to achieve excellent signal-to-noise ratios [27–30]. Time-resolved intrinsic fluorescence lifetime (TRF) detection is an alternative approach that can deconvolve protein species without requiring their chromatographic separation [31]. We have developed a TRF instrument and previously demonstrated its potential for real-time optical deconvolution and monitoring of complex protein mixtures of albumin and ovalbumin [31]. This was achieved using a pulsed laser at 266 nm to excite proteins flowing through a capillary. Intrinsic fluorescence decay

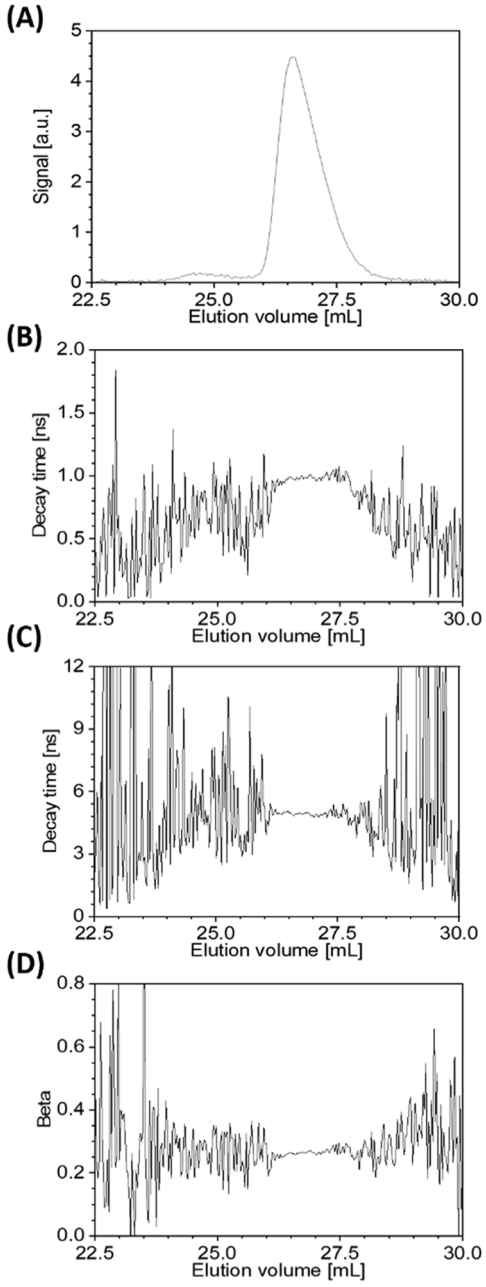

Fig. 2. Chromatograms obtained for an UF eluate using FPLC SEC-TRF. (A) Total fluorescence intensity. Aggregate species eluted at 22.5 to 25.8 mL. Monomer species eluted at 25.9 to 30 mL. The decay parameters obtained for these species as they eluted were the decay times: (B) τ_1 and (C) τ_2, and (D) the β values.

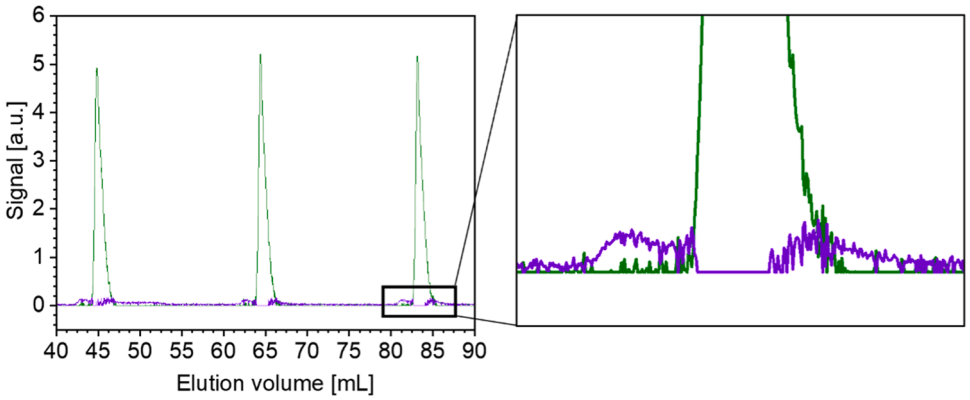

Fig. 3. DAC plots from FPLC SEC-TRF showing the aggregate-fragment SEC chromatogram in purple and the monomer SEC chromatogram in green for the S-Hypercel sample.

profiles on the nanosecond timescale were then obtained in real-time for the protein mixtures. These profiles derived from their respective tryptophan and tyrosine residues, as present in the vast majority of proteins [27], and could be deconvoluted to give decay constants and associated intensities that are characteristics of individual protein species. Here, we explored this approach to deconvolute and quantify the signals from an antibody monomer, from those of the aggregates and fragments present during downstream processing. Our objective was to test the system with three different scenarios: (1) to find the lower and (2) upper, concentration limits of proportionality between the current industrial standard of HPLC-SEC and in-line TRF spectroscopy at its original sensitivity, and then (3), to find the lower concentration bounds of this proportionality using a more sensitive TRF set up with a higher laser pulse power. As the entire signal analysis technique operates on a timescale of seconds to minutes, it has the potential to operate in-line and in real-time, and so eliminates the requirement for running time-consuming off-line or at-line HPLC-SEC during mAb bioprocessing. As we demonstrate here, TRF detection can be used initially in combination with an analytical chromatography column, to map out specific fluorescence decay parameters for all species present in standard samples and in different pH environments. TRF can then be used without an analytical column, to identify and quantify the concentrations of these constituent species within any protein sample, such as those obtained off-line and potentially in-line, from a bioprocess.

2. Experimental methods

2.1. Materials

mAb eluates from Protein A capture chromatography and viral inactivation, cation exchange (CEX) chromatography, anion exchange (AEX) chromatography and ultrafiltration (UF) were provided by Cytiva. The sequence of bioprocess stages from which these samples were sourced is shown in Fig. 1. For the benchmarking of TRF spectroscopy against HPLC-SEC, dilution factors of: 1:2 and 1:3 were applied to samples measured using both techniques, where the viral inactivation, CEX and AEX mAb eluate samples had starting concentrations of 7.0 mg/mL, 6.7 mg/mL and 5.9 mg/mL, respectively. This was to facilitate a comparable SEC chromatogram resolution with TRF spectroscopy and avoid protein overloading of the SEC column. For the more concentrated UF eluate (55.2 mg/mL) sourced from the mAb biomanufacturing line, a 39-fold dilution was applied to generate one UF sample in the *high* concentration range (>1.4 mg/mL). This high concentration range was defined as the point above which direct injection onto the HPLC-SEC column led to saturation effects and lower accuracy in species quantification. An additional eight different UF concentrations at below 1.4 mg/mL were formulated to form a *low* concentration range in the TRF spectroscopy- HPLC-SEC benchmarking. All sample dilutions were performed with the original elution buffer as diluent. Protein concentrations were determined from the mean of three A280 measurements on a NanoDrop 2000 (Thermo Fisher Scientific, USA). All water used in the preparation of the SEC columns and samples was Milli-Q ® (Merck, USA), ultrapure, deionised, and at a resistivity of 18.2 MΩ cm.

2.2. High pressure liquid chromatography

HPLC-SEC of mAb samples was performed with a TSKgel SuperSW3000 SEC column (part number 18675) with a 4 μm pore size, 4.6 mm internal diameter and 30 cm length (Tosoh Bioscience, Japan), using a mobile phase of 0.05 M Sodium Phosphate and 0.4 M Sodium Perchlorate, pH 6.7, degassed after passing through a 0.22 μm filter and vacuum pumped for a minimum of 1 h, or by Helium gas sparging for a minimum of 30 min. HPLC-SEC was used to compare the UV-SEC absorbance peak areas for separated species against decay-associated peak areas for co-eluting species obtained through in-line TRF measurements.

Mobile phase flow regulation and sample injections were performed on the Knauer HPLC system (BIA Separations, Slovenia) together with ClarityChrom software (Knauer, Germany) for system control and to generate chromatograms. UV absorbance was measured at 280 nm with a bandwidth of 8 nm. Analysis times were 30 min for a run at 0.3 mL/min or 60 min for a run at 0.15 mL/min. Samples were injected at 100 μL, after dilutions with their respective bioprocess elution buffers to obtain peak measurements that avoided photodetector saturation. Monomer and aggregate-fragment peak areas were calculated through ClarityChrom, with any peaks preceding the monomer classified as the aggregates, and any peaks following the monomer (retention times: 14–16 min) classified as fragment species. To obtain the concentration-calibration curves samples were injected into the SEC column after 5 column volumes (CVs) of mobile phase.

2.3. Fast protein liquid chromatography with time-resolved fluorescence spectroscopy detection

A Superdex 200 Increase 10/300 GL SEC column (General Electric, USA) was used with an Amersham Biosciences ÄKTA Fast Protein Liquid Chromatography (FPLC) system (Cytiva, USA) to pump injected bioprocess samples into the column at a constant flow rate of 0.3 mL/min. Each sample was run in its respective process elution buffer as a mobile phase: Protein A samples were run with a mobile phase of 20 mM sodium citrate, pH 4.5; CEX samples were run with a mobile phase of 25 mM sodium citrate, 40 mM sodium chloride, pH 6.5; AEX and UF samples were run with a mobile phase of 18.75 mM sodium citrate, 30 mM sodium chloride and 25 mM Tris, pH 7.5. Decay parameters of all samples preceding UF were measured at their original bioprocess

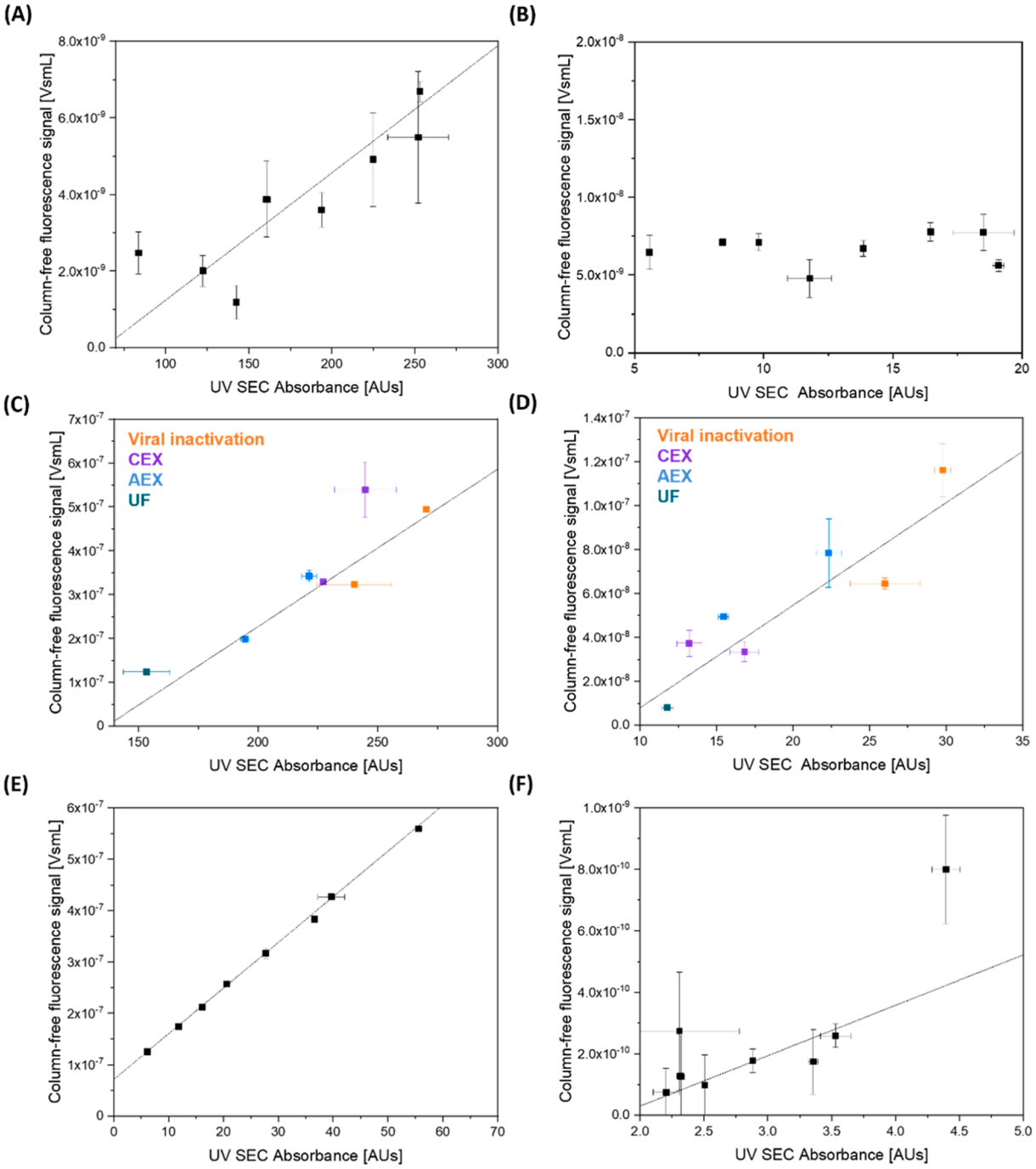

Fig. 4. A–F. Head-to-head analysis of HPLC SEC-UV absorbance species quantification against column-free in-line TRF spectroscopy. Average peak areas ($n = 3$) were plotted against each other for the low concentration UF samples with low laser power (A-B), *high* concentration, low laser power cases (C-D) and *low* concentration AEX samples at high laser power (E-F). Figs. A, C, E are for the monomer and Figs. B, D, and F are for the aggregate/fragment quantification.

concentrations. UF samples were measured after the application of a 1:4 dilution with AEX elution buffer. FPLC SEC-TRF chromatograms allowed fluorescence decay signatures to be obtained for each species where they were resolved into separate peaks. A minimum of 2 CVs of mobile phase was pumped through the SEC column prior to each sample injection. Samples were injected manually into a 100 µL sample loop using sterile Plastipak syringes (BD, USA).

2.4. Time resolved fluorescence spectroscopy

Initial protein-species-dependent parameters for the fluorescence decay measurements were established using FPLC SEC-TRF approach as detailed in 2.3. The decay times τ_1 and τ_2, and the contribution of the first fluorescence decay component β are intrinsic to the protein or protein mixture being quantified and were extracted from regions spanning each peak in SEC chromatograms, after fitting the associated decay lifetime measurements at each elution volume. Plotting the decay parameters as a function of elution volume gave decay chromatograms (DCs) which converged to a set of values with low variance when a specific species was eluting (Fig. S1 Supplementary Information). These decay parameters were used to determine the individual decay intensity contributions of that species to the total fluorescence intensity (Fig. S2

Supplementary Information) [31].

Subsequent measurements were made on the same samples as those evaluated initially by FPLC-SEC, but also on all remaining samples, by direct flow of samples into the TRF detector without an SEC column, as outlined previously [31]. These were injected in-line and pumped through the TRF spectroscopy assembly at 0.3 mL/min. Measurements were made with the TRF spectroscopy assembly in its original sensitivity with a laser pulse power rating of 40 μJ, and separately also in a higher-sensitivity configuration using a higher laser pulse power rating of 50 μJ. Decay-associated chromatogram (DAC) peak traces defining the fluorescence intensity contributions of two species with contrasting decay parameters were generated using the algorithm for analysis of the TRF chromatograph introduced previously [31]. All DAC peak areas were obtained using the *Integrate Gadget* on OriginPro 2019 with a $y = 0$ baseline. Integration windows encompassed the DAC peaks pertaining to each species signal trace. For *high* concentration (>1.41 mg/mL) samples using either the sensitivity-improved or original sensitivity measurements, DAC traces did not require any signal smoothing. For the *low* concentration samples (<1.41 mg/mL), signal smoothing was applied at 5 decays/fitting but only for measurements at the original sensitivity setting (Figs. S3 and S4 Supplementary Information).

3. Results

Our main goal was to demonstrate the potential to use the TRF instrument in-line at various steps in a manufacturing bioprocess, and so we examined samples of mAb taken from different stages, including after: protein-A elution with viral inactivation, S-HyperCel elution, Mustang-Q elution and ultrafiltration. These were first measured in the FPLC SEC-TRF set-up to resolve species peaks and extract their species-specific decay signatures. TRF was then used directly, without a SEC column (direct-TRF) using the previously calculated decay signatures to analyse the quantities of each species. The decay parameters extracted at the point of aggregate elution by SEC were also found to correspond closely to decay intensity contributions of a fragmentary species co-eluting in the descending tail of the monomer peak (Fig. 3), and so the quantity of aggregate and fragment species were measured together with a single set of parameters using direct-TRF. Measurements were then compared to traditional UV absorbance-based peak areas obtained from HPLC-SEC.

The decay parameters for each mAb sample, extracted from the decay chromatograms for each peak in the FPLC SEC-TRF set-up are summarised in Table 1. Fig. 2 demonstrates the convergence of decay parameters towards a narrow set of values for each eluate. Fig. 3 forms an example of the DAC traces obtained from the FPLC SEC-TRF measurements of the mAb monomer (green) and mAb aggregate-fragment (purple) species within the S-HyperCel samples. The purple signal trace was generated using decay parameters obtained from where the aggregates were eluting. Fig. 3 demonstrates that the decay parameters extracted from the decay chromatogram aggregate elution window (Fig. S2 Supplementary Information) yielded DAC traces that could deconvolute the monomer and combined aggregate and fragment species quantities as independent signals, even where in this case the fragment and monomer peaks were overlapping in the FPLC-SEC (Fig. 3).

Measurements were then taken for the same samples, but by flowing them directly into the TRF detector without an SEC column. DAC signals were obtained by deconvoluting the TRF data using the parameters previously obtained from FPLC SEC-TRF and shown in Table 1. Parity plots of the resulting decay intensity derived peak areas, versus the peak areas obtained from HPLC SEC-UV absorbance at 280 nm are shown in Fig. 4 for the mAb monomer, and for the total product-related impurities (aggregate/dimer and fragments).

Measurements were made at both *high* (>1.41 mg/mL) and *low* (<1.41 mg/mL) concentrations with the TRF spectroscopy assembly at its original sensitivity configuration with a "low" laser pulse power rating of 40 μJ. A second set of measurements were also made at increased sensitivity using a "high" laser pulse power rating of 50 μJ for total protein concentrations between 0.28 and 2.82 mg/mL. mAb concentrations were categorised as *high* at >1.41 mg/mL, defined as the point above which saturation of the UV absorbance detector was observed for the monomer peaks in SEC chromatograms.

For measurements taken in the original low sensitivity TRF configuration at *low* mAb concentrations (<1.41 mg/mL), a good correlation and linear relationship with positive slope was observed between the peak areas from HPLC SEC-UV and DAC for the monomer species, with an R^2 of 0.85 and a residual sum of squares (RSS) of 27.34 $[VsmL]^2$(see Fig. 4A). By contrast, no correlation was observed for the aggregate-fragment species peak areas, primarily because the DAC measurements were below the limit of detection (Fig. 4B) in the original low sensitivity TRF configuration.

At higher mAb concentrations (>1.41 mg/mL), the correlations for the monomer and impurity species were both good (at the original low sensitivity TRF setting), with an R^2 of 0.96 and 0.69, respectively (see Fig. 4C and D). The RSS for the linear fit models were 1150 for the monomer and 285 $[VsmL]^2$ for the combined aggregate/fragment species.

At the higher sensitivity TRF setting, the DAC peak areas correlated with the HPLC SEC UV absorbance with an R^2 of 0.999 and an RSS of 27.3 for the monomer species as shown in Fig. 4E. The aggregate/fragment species peak areas at this concentration range gave R^2 and RSS values of 0.64 and 6.6, respectively (see Figs. 4F &, S5 and 6 Supplementary Information).

4. Discussion

The parity plots in Fig. 4 demonstrate that the contributions to the fluorescence intensity from each species measured directly by the TRF instrument without separating them by SEC, are proportional to the 280 nm absorbance peak areas of each species as measured by HPLC-SEC. This suggests that direct TRF detection on samples could be used as an in-line alternative to off-line HPLC-SEC for monitoring protein aggregation.

HPLC-SEC was found to be limited in quantitation of the monomer at higher concentrations (>1.41 mg/ml) due to saturation, observed as peak asymmetry and tailing (eg. in Fig. S7, Supplementary Information). However, the HPLC-SEC UV absorbance measurements on the samples indicated the presence of a detectable antibody fragment species as a distinct peak at 14–16 min (Figs. S7–S12, Supplementary Information). By FPLC-SEC a separate peak could not be resolved, but notably, the decay contribution of the fragment species was now easily detected within the mAb monomer peak tail using the TRF-based decay associated chromatograms (Figs. 3 and S2 Supplementary Information). At the *high* concentrations the HPLC-SEC UV SEC absorbance peaks showed minor tailing and truncation – indicating that total protein concentrations were too high for the column. The subjection of mAbs to high column pressures during HPLC-SEC analysis could also potentially have compounded the degradation and fragmentation pathways further [32]. Each species-specific decay signature identified by FPLC-SEC-TRF likely includes contributions from a broad mix of species including small populations of host-cell proteins. Nonetheless, two signatures can be extracted for which the monomers and aggregates-and-fragments, respectively, are the dominant contributors (Fig. S1 Supplementary Information).

Correlation coefficients obtained from parity plots of HPLC-SEC UV absorbance versus column-free direct-TRF, were strongest for the *high* concentrations with low laser-pulse-power, and also for the high laser-pulse-power configurations. This is due to the proportionalities between excitation pulse power and sample irradiance. An increase in irradiance results in a greater photon flux to the sample, allowing greater fluorescence intensities to be achieved. Greater total protein concentrations correlate with a higher concentration of excitable

fluorophores [33–34], therefore, higher concentrations of aggregate and monomer species would yield greater fluorescence intensities, as would using a higher laser pulse power. Lower concentrations generate signals closer to the noise floor. Lower signal-to-noise ratios resulted in greater portions of the decay intensity contributions being attributable to noise, which would explain the reduction in the correlation coefficient for the *low* concentrations. Dilutions had to be applied to both sample sets injected through the TRF spectroscopy and HPLC-SEC systems to generate comparable analyses. However, the dilution of intermediate bioprocess samples from Protein-A to AEX is not required if analysing through TRF spectroscopy.

These results show that the laser-pulse power ratings can be varied in order to quantify species across different concentration ranges. Higher powers might therefore be used specifically to detect aggregates or fragments, while lower powers might be preferred for monomer quantification with minimal probability of photobleaching or UV-damage during in-line monitoring. The options of DAC signal smoothing and baseline noise signal removal are also available for lower concentrations (<1.41 mg/mL) to generate a good correlation between TRF spectroscopy and HPLC-SEC. However, these results were a strong indicator that the sensitivity of the TRF chromatographs would be sufficient for bioprocessing applications where typical total protein concentrations range from ~5 mg/mL to ~10 mg/mL in downstream purification. With the improved sensitivity configuration, we have found that accuracy-reducing smoothing techniques do not need to be applied for concentrations at and above 0.28 mg/mL. For even higher concentration applications, such as those requiring the measurement of UF eluates, a neutral-density filter positioned between the sample and the detector could be used to attenuate emission intensities that would otherwise cause detector saturation [35]. This would allow the system to accurately record fluorescence intensities for undiluted protein concentrations at the desired bioprocess stages. The increases to protein throughput, titres and yields desired by industry, would increase the signal-to-noise ratios and quantification accuracies offered by TRF detection. These results therefore set the foundations for validating SEC-free TRF detection for industrial CQA monitoring in mAb biomanufacture from post-Protein A capture to between each purification step, and post-polishing/formulation.

Overall, the results in this paper demonstrate that SEC-free TRF detection can monitor the total product impurity in-line and quantify mAb in a mixture consisting of monomers, aggregates and fragments. Its freedom from mobile-phase related constraints would allow it to be integrated into any stage of the downstream process and run as an in-line analysis of process/product-related impurities, resulting in a more rapid evaluation of capture and purification efficiency. One particular advantage of TRF will be in the real-time optical deconvolution of chromatography peaks for which the monomer and aggregate or fragment species are not physically separated. Overall, this rapid deconvolution of monomer from product-related contaminants will bring a firmer Quality-by-Design approach to production with a deeper understanding of the influence of each process stage on the product's critical quality attributes.

CRediT authorship contribution statement

Deniz Uçan: Conceptualization, Methodology, Validation, Investigation, Writing – review & editing. **John E. Hales:** Conceptualization, Methodology, Software, Validation, Formal analysis, Investigation, Data curation, Writing – original draft, Writing – review & editing, Visualization. **Samir Aoudjane:** Methodology, Validation, Investigation, Writing – review & editing. **Nathan Todd:** Conceptualization, Writing – review & editing, Funding acquisition. **Paul A. Dalby:** Conceptualization, Methodology, Validation, Writing – review & editing, Supervision, Project administration, Funding acquisition.

Declaration of Competing Interest

The authors declare the following financial interests/personal relationships which may be considered as potential competing interests: J. E.H. and P.A.D. are co-authors on a patent application which could increase in value if the methods and ideas described in this paper find widespread application.

Data availability

Data will be made available on request.

Acknowledgments

This work was supported by the Engineering and Physical Sciences Research Council (EPSRC EP/N025105/1, EP/P006485/1, EP/X025446/1), an EPSRC Future Leaders Fellowship (MR/T02156X/1) and via an EPSRC Doctoral Studentship for DU (EP/S021868/1). The doctoral researcher (DU) was co-supported by Cytiva. The funding sources had no involvement in the study design, in the collection, analysis and interpretation of data, in the writing of the report, or in the decision to submit the article for publication.

Supplementary materials

Supplementary material associated with this article can be found, in the online version, at doi:10.1016/j.chroma.2023.464463.

References

[1] H. Kaplon, M. Muralidharan, Z. Schneider, J.M. Reichert, Antibodies to watch in 2020, mAbs 12 (2020), 1703531.
[2] B.A. Teicher, R.V. Chari, Antibody conjugate therapeutics: challenges and potential, Clin. Cancer Res. 17 (2011) 6389–6397.
[3] N. Alt, T.Y. Zhang, P. Motchnik, R. Taticek, V. Quarmby, T. Schlothauer, H. Beck, T. Emrich, R.J. Harris, Determination of critical quality attributes for monoclonal antibodies using quality by design principles, Biologicals 44 (2016) 291–305.
[4] M.E. Cromwell, E. Hilario, F. Jacobson, Protein aggregation and bioprocessing, AAPS J. 8 (2006) E572–E579.
[5] A.R. Mazzer, X. Perraud, J. Halley, J. O'Hara, D.G. Bracewell, Protein A chromatography increases monoclonal antibody aggregation rate during subsequent low pH virus inactivation hold, J. Chromatogr. A 1415 (2015) 83–90.
[6] A.A. Shukla, P. Gupta, X. Han, Protein aggregation kinetics during protein A chromatography. Case study for an Fc fusion protein, J. Chromatogr. A 1171 (2007) 22–28.
[7] J. Vlasak, R. Ionescu, Fragmentation of monoclonal antibodies, mAbs 3 (2011) 253–263.
[8] T. Xiang, E. Lundell, Z. Sun, H. Liu, Structural effect of a recombinant monoclonal antibody on hinge region peptide bond hydrolysis, J. Chromatogr. B 858 (2007) 254–262.
[9] H. Sandberg, D. Lutkemeyer, S. Kuprin, M. Wrangel, A. Almstedt, P. Persson, V. Ek, M. Milkaelsson, Mapping and partial characterization ofproteases expressed by a CHO production cell line, Biotechnol. Bioeng. 95 (2006) 961–971.
[10] S.X. Gao, Y. Zhang, K. Stansberry-Perkins, A. Buko, S. Bai, V. Nguyen, M.L. Brader, Fragmentation of a highly purified monoclonal antibody attributed to residual CHO cell protease activity, Biotechnol. Bioeng 108 (2011) 977–982.
[11] H.J. Lee, C.M. Lee, K. Kim, J.M. Yoo, S.-M. Kang, G.-S. Ha, M.K. Park, M.-A. Choi, B.L. Seong, D.E. Lee, Purification of antibody fragments for the reduction of charge variants using cation exchange chromatography, J. Chromatogr. B 1080 (2018) 20–26.
[12] G. Rodrigo, M. Gruvegård, J. Van Alstine, Antibody fragments and their purification by protein L affinity chromatography, Antibodies 4 (2015) 259–277.
[13] H.-N. Song, J.-H. Jang, Y.-W. Kim, D.-H. Kim, S.-G. Park, M.K. Lee, S.-H. Paek, E.-J. Woo, Refolded scFv antibody fragment against myoglobin shows rapid reaction kinetics, Int. J. Mol. Sci. 15 (2014) 23658–23671.
[14] T.M. Dillon, P.V. Bondarenko, D.S. Rehder, G.D. Pipes, G.R. Kleemann, M.S. Ricci, Optimization of a reversed-phase high-performance liquid chromatography/mass spectrometry method for characterizing recombinant antibody heterogeneity and stability, J. Chromatogr. A 1120 (2006) 112–120.
[15] J.P. Gabrielson, M.L. Brader, A.H. Pekar, K.B. Mathis, G. Winter, J.F. Carpenter, T. W. Randolph, Quantitation of aggregate levels in a recombinant humanized monoclonal antibody formulation by size-exclusion chromatography, asymmetrical flow field flow fractionation, and sedimentation velocity, J. Pharm. Sci. 96 (2007) 268–279.

[16] H. Pan, K. Chen, M. Pulisic, I. Apostol, G. Huang, Quantitation of soluble aggregates in recombinant monoclonal antibody cell culture by pH-gradient protein A chromatography, Anal. Biochem. 388 (2009) 273–278.
[17] J.C. Rea, G.T. Moreno, L. Vampola, Y. Lou, B. van Haan, G. Tremintin, L. Simmons, A. Nava, Y.J. Wang, D. Farnan, Capillary size exclusion chromatography with picogram sensitivity for analysis of monoclonal antibodies purified from harvested cell culture fluid, J. Chromatogr. A 1219 (2011) 140–146.
[18] A.J. Paul, K. Schwab, F. Hesse, Direct analysis of mAb aggregates in mammalian cell culture supernatant, BMC Biotechnol. 14 (2014) 99.
[19] E. Krayukhina, S. Uchiyama, K. Nojima, Y. Okada, I. Hamaguchi, K. Fukui, Aggregation analysis of pharmaceutical human immunoglobulin preparations using size-exclusion chromatography and analytical ultracentrifugation sedimentation velocity, J. Biosci. Bioeng. 115 (2013) 104–110.
[20] T.;. Arakawa, D. Ejima, T. Li, J.S. Philo, The critical role of mobile phase composition in size exclusion chromatography of protein pharmaceuticals, J. Pharm. Sci. 99 (2010) 1674–1692.
[21] M. Rüdt, T. Briskot, J. Hubbuch, Advances in downstream processing of biologics – spectroscopy: an emerging process analytical technology, J. Chromatogr. A 1490 (2017) 2–9.
[22] S. Arase, K. Horie, T. Kato, A. Noda, Y. Mito, M. Takahashi, T. Yanagisawa, Intelligent peak deconvolution through in-depth study of the data matrix from liquid chromatography coupled with a photo-diode array detector applied to pharmaceutical analysis, J. Chromatogr. A 1469 (2016) 35–47.
[23] N. Brestrich, T. Briskot, A. Osberghaus, J. Hubbuch, A tool for selective inline quantification of co-eluting proteins in chromatography using spectral analysis and partial least squares regression, Biotechnol. Bioeng. 111 (2014) 1365–1373.
[24] N. Brestrich, A. Sanden, A. Kraft, K. McCann, J. Bertolini, J. Hubbuch, Advances in inline quantification of co eluting proteins in chromatography: process data based model calibration and application towards real life separation issues, Biotechnol. Bioeng. 112 (2015) 1406–1416.
[25] N. Brestrich, M. Rüdt, D. Büchler, J. Hubbuch, Selective protein quantification for preparative chromatography using variable pathlength UV/Vis spectroscopy and partial least squares regression, Chem. Eng. Sci. 176 (2018) 157–164.
[26] S.K. Hansen, B. Jamali, J. Hubbuch, Selective high throughput protein quantification based on UV absorption spectra, Biotechnol. Bioeng. 110 (2013) 448–460.
[27] A.T. Timperman, K.E. Oldenburg, J.V. Sweedler, Native fluorescence detection and spectral differentiation of peptides containing tryptophan and tyrosine in capillary electrophoresis, Anal. Chem. 67 (1995) 3421–3426.
[28] J. Roegener, P. Lutter, R. Reinhardt, M. Blüggel, H.E. Meyer, D. Anselmetti, Ultrasensitive detection of unstained proteins in acrylamide gels by native UV fluorescence, Anal. Chem. 75 (2003) 157–159.
[29] Z. Zhu, M. Lies, J. Silzel, Native fluorescence detection with a laser driven light source for protein analysis in capillary electrophoresis, Anal. Chim. Acta 1183 (2021), 338936.
[30] J. Xue, Y. Cao, G. Zha, Z. Yu, Y. Wang, W. Liu, J. Ren, H. Xiao, Q. Zhang, L. Wei, C. Cao, Quadruple UV LED array for facile, portable, and online intrinsic fluorescent imaging of protein in a whole gel electrophoresis chip, Anal. Chem 95 (2023) 6193–6197.
[31] J.E. Hales, S. Aoudjane, G. Aeppli, P.A. Dalby, Proof-of-concept analytical instrument for label-free optical deconvolution of protein species in a mixture, J. Chromatogr. A 1641 (2021), 461968.
[32] S. Fekete, K. Ganzler, D. Guillarme, Critical evaluation of fast size exclusion chromatographic separations of protein aggregates, applying sub-2μm particles, J. Pharma. Biomed. Anal. 78-79 (2013) 141–149.
[33] Edited by M.R.S. McCoustra, D.L. Andrews, A.A. Demidov, Methods, diagnostics and instrumentation, Introduction to Laser Spectroscopy (1995) 19–33. Edited byNew York.
[34] L. Nouchikian, C. Roque, J.Y. Song, N. Rahman, S.F. Ausar, An intrinsic fluorescence method for the determination of protein concentration in vaccines containing aluminum salt adjuvants, Vaccine 36 (2018) 5738–5746.
[35] J.E. Hales, G. Matmon, P.A. Dalby, J.M. Ward, G. Aeppli, Virus lasers for biological detection, Nature Comms 10 (2019) 3594.